HOKKAIDO UNIVERSITY

Title	Colloidal platinum nanoparticles enhance resin-dentin bonding durability
Author(s)	Yuan, Yuan; Intajak, Papichaya; Sakaguchi, Norihito et al.
Citation	Dental materials, 40(11), 2034-2042 https://doi.org/10.1016/j.dental.2024.09.015
Issue Date	2024-11
Doc URL	https://hdl.handle.net/2115/96047
Rights	© 2024. This manuscript version is made available under the CC-BY-NC-ND 4.0 license http://creativecommons.org/licenses/by-nc-nd/4.0/
Rights(URL)	https://creativecommons.org/licenses/by-nc-nd/4.0/
Type	journal article
File Information	yuan manuscript for DM.pdf

Hokkaido University Collection of Scholarly and Academic Papers : HUSCAP

Abstract

Objectives: This study aims to investigate the effect of colloidal platinum nanoparticles (CPN) on the durability of resin-dentin bonding performance with contemporary adhesives.

Methods: Sixty non-carious human maxillary premolars were subjected to microtensile bond strength (μTBS) testing and divided into two main groups: CPN-treated and untreated. Within each group, specimens were randomly allocated to Clearfil Megabond 2 (MB2), Scotchbond Universal Plus Adhesive with self-etch mode (SE-SUP), and etch-and-rinse mode (ER-SUP) subgroups (n = 10/group). CPN was applied to dentin in the MB2 and SE-SUP groups for 20 seconds, followed by rinsing before adhesive application. In the ER-SUP group, CPN was applied after etch-and-rinse. The μTBS was tested after 24 hours, 6 months, and 1 year, and the fracture modes were observed using SEM. The μTBS data were analyzed using a two-way ANOVA and post-hoc Tukey HSD test (α = 0.05). An additional twelve premolars underwent TEM/STEM/EDX for ultra-morphological observations.

Results: The application of CPN significantly prevented a decline in the μTBS of both the MB2 and SE-SUP groups. No significant decrease was observed in the ER-SUP group,

either with aging or CPN application. Ultra-morphological images revealed platinum nanoparticles attaching to the collagen fibrils of the hybrid layer regardless of aging. It was highlighted that the nanoparticles attached to the banded collagen in the aging groups were observed.

Significance: CPN exhibits the potential in enhancing the longevity of resin-dentin bonding in SE mode.

Keywords: nanomaterials, hydrolysis, adhesive, longevity, collagen, energy dispersive x-ray spectroscopy, transmission electron microscopy

1. Introduction

In the field of restorative dentistry, the effectiveness of resin-dentin bonds is crucial to the success of dental restorations. A reliable resin-dentin bond depends on the quality of the "hybrid layer" [1]. This nanointeraction zone not only influences the immediate structural integrity of restorations but also has a significant impact on long-term restoration performance [2]. Adhesive dentistry has rapidly evolved in recent decades, with current dentin adhesives achieving satisfactory initial bond performance [3]. The two-step self-etch adhesive Clearfil Megabond 2 (the Japanese version of Clearfil SE 2), is still regarded as the gold standard for the self-etch strategy in both laboratory and clinical settings. Numerous studies have consistently shown its excellent initial bond performance, attributed to the separate application of the hydrophilic primer and hydrophobic bond, as well as the highly effective functional monomer 10-MDP [4, 5]. Nowadays, the all-in-one adhesive system, classified as a universal adhesive, has been widely used due to its versatility in application to various substrates and multi-mode adhesion strategies. Universal adhesives appear to exhibit acceptable immediate dentin bonding capabilities, whether employed in self-etch or etch-and-rinse mode [6]. Nevertheless, resin-dentin bonding durability remains a significant challenge, whether employing a two-step self-etch adhesive or a universal adhesive, as it depends on the deterioration of the hybrid

layer [7, 8].

Nanomaterials, originating from natural or manufactured, comprise 50% or more of particles confined within the size range of approximately 1–100 nm [9]. At this nanoscale, nanoparticles exhibit novel properties and functions distinct from those observed at the bulk scale, with the potential for significant impacts in industry, medicine, and the natural sciences [10]. Additionally, the applications of nanoparticles in dentistry have increased, driven by their antibacterial action, and physical, mechanical, and biological characteristics [11, 12].Colloidal platinum nanoparticles (CPN) represent a suspension of nanosized platinum particles stabilized with a protective agent [13]. This synthesized nanomaterial stands out as a potent quencher of reactive oxygen species, essentially exhibiting impressive antioxidant characteristics [14, 15]. Various pieces of evidence in the medical field have demonstrated CPN's efficacy in mitigating inflammation, preventing apoptosis, and inhibiting metalloproteinase [16, 17, 18, 19]. Beyond its medical applications, recent studies have revealed the antibacterial activity of CPN against *S. mutans* and its ability to inhibit biofilm formation in dentistry [20, 21]. Moreover, CPN has been proven to enhance immediate bond strength in the intricate process of dentin bonding with 4-META/MMA-TBB resin as a dental primer [22]. However, few studies have assessed the impact of CPN on the mechanical properties of

contemporary adhesives, leaving a gap in understanding the influence of CPN on the durability of the resin-dentin interface.

Therefore, the aim of this in vitro study was to investigate the effect of CPN on the durability of resin-dentin bonding performance with current adhesives. The null hypothesis tested were: (1) the application of CPN would not affect the bonding durability, and (2) the bond strength of each adhesive would not decrease with aging.

2. Materials and Methods

2.1. Tooth preparation and bonding procedure

The research ethics committee of the Graduate School of Dental Medicine at Hokkaido University approved this study (approval number 2018-7). Seventy-two non-carious human maxillary premolars, extracted for orthodontic reasons with the informed consent of the patients, were used for this study. They were stored in a 0.5% chloramine-T solution at 4°C and used within 6 months of storage.

Sixty extracted non-carious human maxillary premolars were used for the μTBS test. The mid-coronal dentin surface was exposed by grinding the occlusal enamel with a gypsum model trimmer. Subsequently, the dentin surface was manually ground with 600-grit SiC paper (Sankyo-Rikagaku, Saitama, Japan) under running water for 1 minute to create a

smear layer. All the teeth were categorized into two main groups: one receiving CPN (0.02wt% platinum, 0.29wt% sodium citric acid, 99.69wt% water; Apt, Tokyo, Japan) application [CPN(+)] and the other without CPN application [CPN(-)]. Each group was further subdivided into three subgroups: Clearfil Mega BOND 2 (MB2; Kuraray Noritake, Tokyo, Japan), Scotchbond Universal Plus Adhesive in self-etch mode (SE-SUP; 3M, Seefeld, Germany), and etch-and-rinse mode (ER-SUP). In the MB2 and SE-SUP groups, CPN was applied to the dentin for 20 seconds, followed by rinsing with distilled water for 10 seconds before adhesive application. In the ER-SUP group, the dentin surface was etched with 35% phosphoric acid (Ultra-Etch™ J; Ultradent Products, INC., South Jordan, UT, USA) for 15 seconds, rinsed with distilled water for 10 seconds, and then treated with CPN as described above. The adhesive application followed the manufacturers' instructions. Then all bonded surfaces were restored with two layers of 2-mm-thick resin composite (Clearfil AP-X; Kuraray Noritake) and light-cured. All the specimens were stored in distilled water at 37℃ for 24 hours.

2.2. μTBS test and fracture mode analysis

After 24 hours storage, resin-dentin sticks (cross-sectional area: 1 ± 0.05 mm^2) were prepared using a low-speed diamond saw (IsoMet 1000, Buehler; Lake Bluff, IL, USA) according to the non-trimming technique. The bonded sticks, originating from the same

teeth, were randomly divided and assigned for testing immediately, as well as after 6 months and 1 year of storage in distilled water at 37°C. The sticks were affixed to a Ciucchi's jig using cyanoacrylate glue (Model Repair 2 Blue; J. Morita, Osaka, Japan) and subjected to tensile forces at a crosshead speed of 1 mm/min in a desktop testing apparatus (EZ-S; Shimadzu, Kyoto, Japan) until failure occurred. Bond strength was expressed in MPa. The mean bond strength of three sticks derived from each tooth represented the μTBS of that tooth, generating 10 values for each tested group [23,24]2017,Armstrong S; 2020,Sano H.

After testing, the fractured specimens were carefully removed from the jigs and mounted on aluminum stubs. The fracture modes of the specimens were visualized using a light microscope (×20 magnification; Magnifier Light, Asone, Osaka, Japan). They were then coated with Pt-Pd for 120 seconds and confirmed by scanning electron microscopy (SEM; S-4000, Hitachi, Tokyo, Japan) at an accelerating voltage of 10 kV. Failure modes on the dentin sides of specimens were taken into consideration and classified as follows: mixed failure, adhesive failure, cohesive failure in dentin, and cohesive failure in resin composite [23].

2.3. Specimen preparation for TEM/STEM and EDX analysis

An additional twelve maxillary premolars were used for transmission electron microscopy (TEM) analysis of the adhesive-dentin interface. The tooth preparation and bonding procedures were conducted in the same manner as previously described. The resin-dentin sticks were processed for TEM according to the procedure described in previous studies [23]. Subsequently, the ultrathin sections were observed by TEM (JEM-1400Plus; JEOL, Tokyo, Japan) and further detected by Cs-corrected Scanning Transmission Electron Microscope (STEM; Titan3 G2 60-300, FEI, Hillsboro, OR, US) with energy dispersive X-ray (EDX) at an accelerating voltage of 80kV.

2.4. Statistical analysis

The statistical analysis was conducted using the SPSS software package (SPSS version 25; IBM, Armonk, NY, USA). The normal distribution was assessed using the Shapiro-Wilk test, and the homogeneity of variance was evaluated using Levene's test. Based on the results of these tests, the μTBS data from the MB2, SE-SUP, and ER-SUP groups were subjected to a two-way ANOVA, considering two factors: CPN application and aging (24-hour, 6-month, and 1-year). An interaction effect between these two factors was observed in the MB2 and SE-SUP groups ($P < 0.05$). Consequently, a Tukey test was conducted separately for the MB2, SE-SUP, and ER-SUP groups ($\alpha = 0.05$).

3. Results

3.1. Microtensile bond strength

The results of the μTBS are presented separately for the MB2, SE-SUP, and ER-SUP groups (Fig. 1A). In the MB2 group, a two-way ANOVA revealed that CPN application ($P < 0.05$) and aging ($P < 0.05$), as well as their interaction ($P < 0.05$), significantly influenced the μTBS. The μTBS showed no significant difference at 24 hours and 6 months, but a significant decrease was observed at 1 year in the CPN(-) group. In the SE-SUP group, a two-way ANOVA revealed that CPN application ($P < 0.05$), aging ($P < 0.05$), and their interaction ($P < 0.05$) significantly influenced the μTBS. In the CPN(-) groups, the μTBS of SE-SUP showed a significant decrease at 6 months and 1 year. However, in the CPN(+) group, no significant difference was observed in μTBS among the 24-hour, 6-month, and 1-year periods in both the MB2 and SE-SUP groups. For the ER-SUP group, the two-way ANOVA indicated that there was no statistically significant effect of CPN application on the μTBS ($P > 0.05$). Additionally, the interaction between CPN application and aging was not significant ($P > 0.05$). No significant differences were found among all the groups in the ER-SUP analysis ($P > 0.05$).

3.2. Failure modes analysis

The frequency distribution of failure modes is presented separately for the MB2, SE-SUP, and ER-SUP groups (Fig. 1B). There was no pre-test failure in this study. In the MB2 and SE-SUP groups, adhesive failure was more likely to occur in the adhesive layer rather than the hybrid layer in the CPN(+) subgroup. In the ER-SUP group, the primary failure mode was cohesive dentin failure in the CPN(+) subgroup, irrespective of aging.

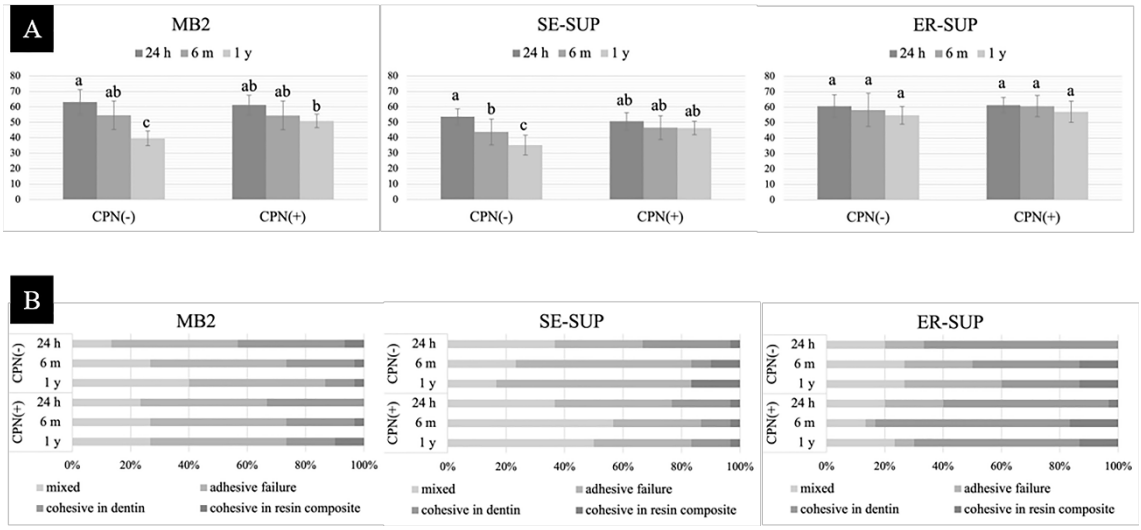


Figure 1. Mean (Standard deviation) of μTBS and frequency distribution of failure modes for each group. (A) The μTBS data of Clearfil Megabond 2 (MB2), Scotchbond Universal Plus Adhesive with self-etch mode (SE-SUP), and etch-and-rinse mode (ER-SUP) were presented in separate graphs. Groups labeled with different lowercase letters showed significant differences ($P < 0.05$, n = 10 teeth). (B) The percentage distribution of failure modes for MB2, SE-SUP, and ER-SUP groups. In the MB2 group, the predominant failure mode is mixed failure. Adhesive mixing with dentin failure increased with aging in the

CPN(-) subgroup while adhesive mixing with resin composite increased with aging in the CPN(+) subgroup. In the SE-SUP group, adhesive failure increased with aging in the CPN(-) subgroup, whereas mixed failure increased with aging in the CPN(+) subgroup. In the ER-SUP group, adhesive failure increased with aging in the CPN(-) subgroup but exhibited a declining trend in the CPN(+) subgroup.

3.3. TEM interface characterization

The ultramorphological characterization of the adhesive-dentin interface is separately shown for the MB2, SE-SUP, and ER-SUP groups (Fig. 2-4). The platinum nanoparticle deposition can be observed along the hybrid layer in all the CPN(+) groups.

In the MB2 group, CPN(-) subgroup exhibited a tight interface in the 24-hour specimens, with hydroxyapatite crystals dispersed throughout the interaction zone (Fig. 2A, B). After 6 months, adhesive fillers were absent near the hybrid layer, and spaces between collagen fibrils were observed (Fig. 2C, D). Additionally, collagen fibrils were unraveled after 1 year (Fig. 2E, F). In the CPN(+) subgroup, platinum nanoparticles attached to the exposed collagen fibrils were observed regardless of aging (Fig. 2a-f). Notably, platinum nanoparticles attached to collagen fibrils were observed. Furthermore, these collagen

fibrils exhibited an intact structure, clearly revealing a cross-banding pattern (Fig. 2e, f).

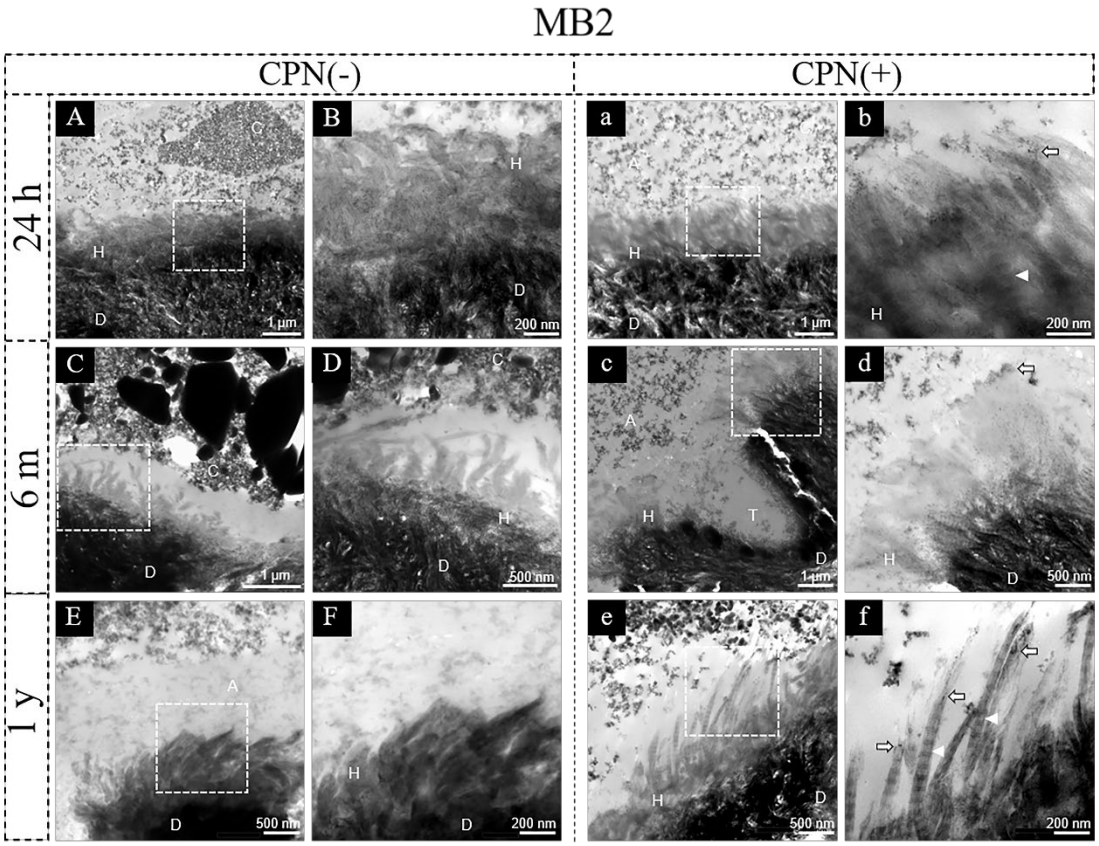


Figure 2. Transmission-electron microscopy images of Clearfil Megabond 2 (MB2). Non-demineralized, stained sections illustrated the resin-detin interface of MB2 after 24 hours, 6 months, and 1 year of water storage. An approximately 500 nm to 1 μm thick shag-carpet hybrid layer was observed in all the images. In the CPN(-) group, a tight interface was observed, and hydroxyapatite crystals were dispersed throughout the interaction zone in 24-hour specimens (**A**, **B**); after 6 months, the fillers of adhesive were absent near the hybrid layer side, and wide spaces were observed between the collagen fibrils (**C**, **D**); collagen fibrils were unraveled after 1 year (**E**, **F**). In the CPN(+) group,

platinum nanoparticles (white arrow) attached to the exposed collagen fibers were observed in all images (**a~f**); the banded collagen fibrils, which attached with platinum nanoparticles (arrow-head) were visible after 1 year (**f**). A: adhesive; C: resin composite; D: dentin; H: hybrid layer; T: dentinal tubule.

In the SE-SUP group, CPN(-) subgroup revealed the presence of hydroxyapatite in the partially demineralized nanohybrid layer in 24-hour specimens, while aging specimens exhibited an obscured hybrid layer. Furthermore, the absence of adhesive fillers was observed on the hybrid layer in the 6-month specimens (Fig 3C, D). Additionally, the composite fillers near the interface were also absent after 1 year (Fig. 3E, F). In the CPN(+) subgroup, platinum nanoparticles were observed to deposit along the exposed collagen fibrils of the hybrid layer regardless of aging (Fig. 3a-f). Despite the partial absence of adhesive fillers over time, the hybrid layer still maintained its integrity (Fig. 3d, f).

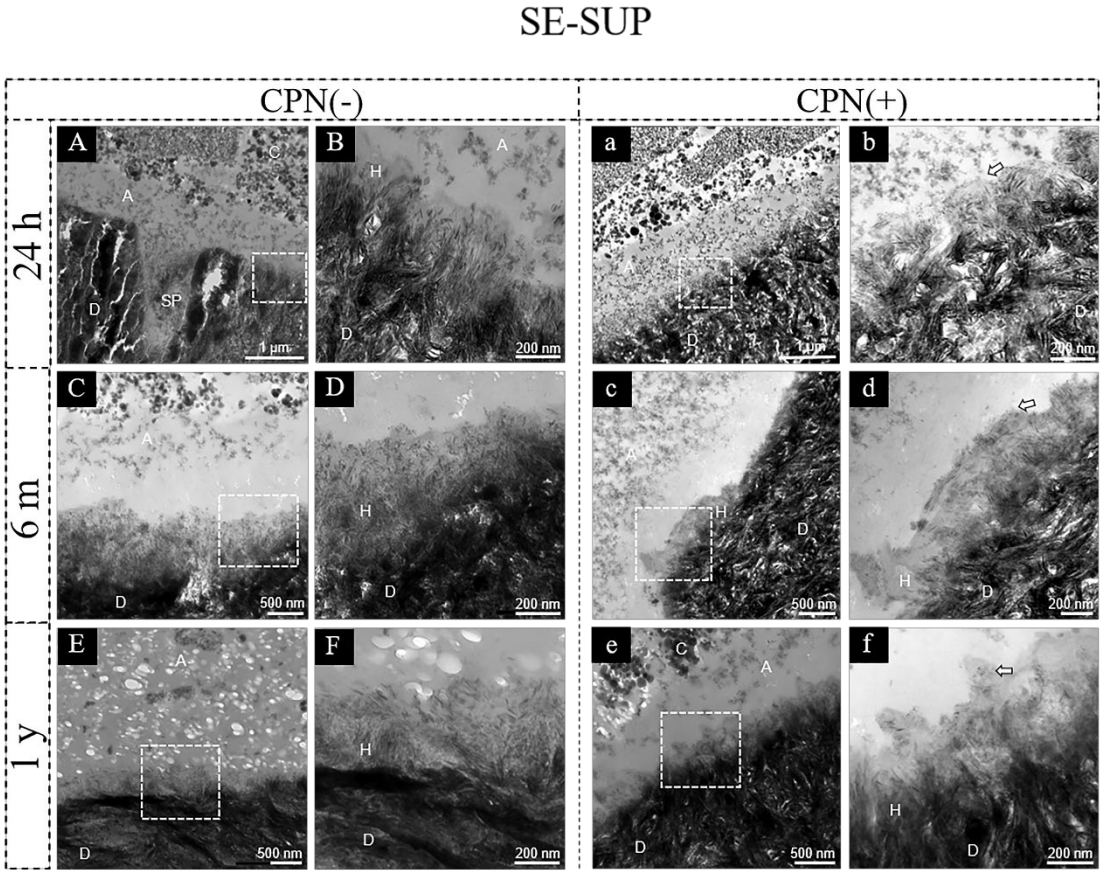


Figure 3. Transmission-electron microscopy images of Scotchbond Universal Plus Adhesive (SUP) with SE mode. Non-demineralized, non-stained sections illustrated the resin-detin interface after 24 hours, 6 months, and 1 year of water storage. An approximately 200 nm thick hybrid layer was observed in all the images. In the CPN(-) group, the smear plug was observed in the dentin tubular (**A**); the hybrid layer appeared obscured, and fillers on the hybrid layer were absent after 6 months (**C**, **D**); furthermore, the filler-absent zone was enlarged after 1 year (**E**, **F**). In the CPN(+) group, platinum nanoparticles (white arrow) attached to the exposed collagen fibers were observed in all

images (**a~f**). A: adhesive; C: resin composite; D: dentin; H: hybrid layer; SP: smear plug.

In the ER-SUP group, an intact hybrid layer was revealed in all groups, irrespective of aging. Staining of cross-banding collagen fibrils in the demineralized zone was still observable in aging specimens. Platinum nanoparticles densely attached to the collagen fibrils regardless of aging in the CPN(+) subgroup (Fig. 4a-f).

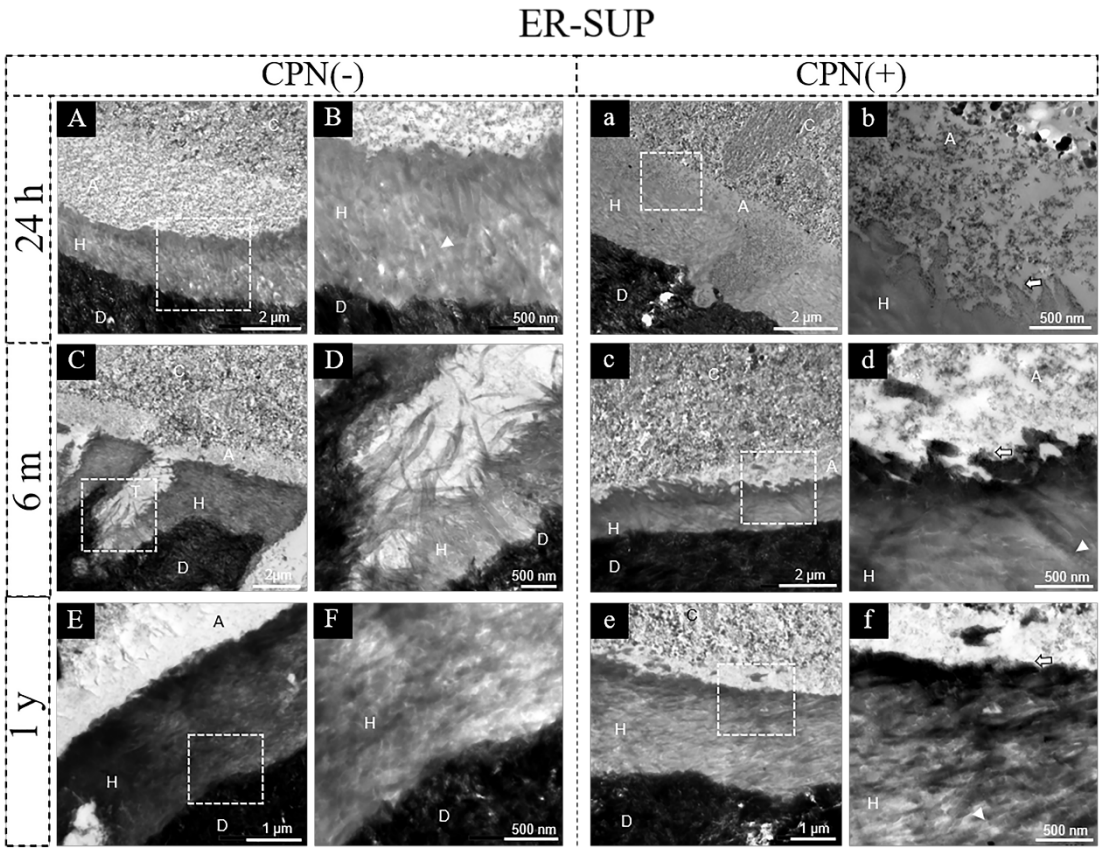


Figure 4. Transmission-electron microscopy images of Scotchbond Universal Plus Adhesive (SUP) with ER mode. Non-demineralized, stained sections illustrated the resin-

detin interface of SUP after 24 hours, 6 months, and 1 year of water storage. An approximately 2 to 3 μm thick hybrid layer was shown in all the images. The smear layer and smear plug were completely removed, allowing the nanofillers of adhesive to infiltrate into the dentin tubular (**C**, **D**). The intact collagen fiber morphology was still visible after 6 months (**d**), and 1 year (**f**), and banded collagen fibrils (arrow-head) were observed. Platinum nanoparticles (white arrow) attached to the exposed collagen fibers were observed in all images of CPN(+) group (**a~f**). A: adhesive; C: resin composite; D: dentin; H: hybrid layer; T: dentinal tubule.

3.4. Cs-corrected TEM and EDX analysis

The ultramorphological images of ER-CPN-SUP at 6 months are shown (Fig. 5). The EDX mapping detected nanoparticles, identified as platinum, distributed along the exposed collagen fibrils of the hybrid layer (Fig 5A, B, C). Furthermore, the nanoparticles infiltrated into the dentinal tubule and deposited along the demineralized peritubular dentin.

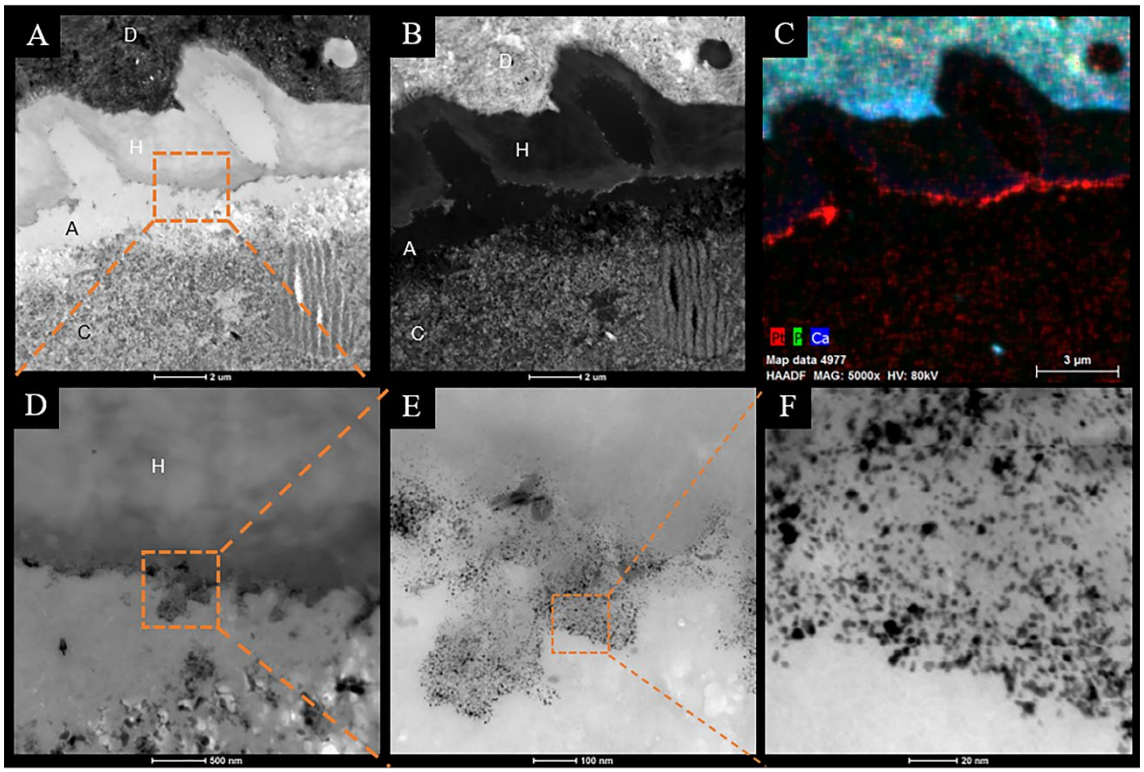


Figure 5. STEM-EDX images of the resin-dentin interface of ER-SUP CPN(+) at 6 months. The interface images were presented in Bright Field (**A**) and High-Angle Annular Dark Field (**B**) at 5k×magnification. EDX mapping revealed the deposition of Pt (red color) along the demineralized surface, with the Ca (blue color) and P (green color) elements overlapping, indicating their presence as the main components of dentin (**C**). The higher magnification images (**D**, 20k×; **E**, 80k×; **F**, 450k×) revealed the distribution of platinum nanoparticles, with an average size around 2 to 3 nm. A: adhesive; C: resin composite; D: dentin; H: hybrid layer.

4. Discussion

Previous research has demonstrated the superior antioxidant and antibacterial properties of CPN, and this study aims to further explore its efficacy in restorative dentistry. No significant difference was found between the CPN(-) and CPN(+) groups in terms of initial bond strength in our study. This is likely due to the excellent initial bond performance achieved by both MB2 and SUP [3]. However, in the CPN(-) group, the bond strength of MB2 significantly decreased after 1 year, and the bond strength of SE-SUP exhibited significant decreases at both 6 months and 1 year. Conversely, the CPN(+) group revealed no significant deterioration during the aging process. On the other hand, the μTBS of SUP in ER mode did not exhibit a significant decrease in either the aging process or with CPN application. Therefore, both null hypotheses were rejected in this study.

In this study, TEM images revealed that MB2 exhibited a typical shag-carpet smear-hybrid layer around 0.5 to 1 μm, which is relatively thicker than the 200-nm-thick smear-hybrid layer observed in SUP in SE mode, in line with previous findings [24]. One reason for this difference may be attributed to the pH variation, as MB2 (pH≅2.0) follows a mild self-etch approach, while SUP (pH≅3.0) adopts an ultra-mild self-etch approach (pH was measured in this study but not shown in the results). Another reason may be due to the

different purity of the functional monomer MDP [25]. In the present study, we observed a significant decrease in bond strength after 1 year in the MB2 CPN(-) group, along with the findings of previous studies that highlighted the occurrence of hydrolysis in the hybrid layer of dentin bonds under water storage conditions [26, 27]. Additionally, TEM ultramorphology of the resin-dentin interface revealed wide interfibrillar spaces between the collagen fibrils, and banded collagen fibrils were unraveled with aging (Fig. 2E, F), further indicating the occurrence of hybrid layer degradation.

There have been numerous studies on the bonding performance of Scotchbond Universal adhesive (SBU) in both SE and ER modes [28, 29, 30, 31]. However, there has been limited research on dentin bonds with the new bottle (SUP). Our study is the first to investigate the aging of dentin bonds with SUP in both SE and ER modes. In the SE-SUP group, TEM images revealed the absence of adhesive silica fillers, and cohesive failure within the adhesive resin increased at 6 months, contributing to the significant decline in bond strength. Furthermore, the subsequent enlargement of the filler-absent area was observed at 1 year. This phenomenon may be due to the water-containing adhesive and the osmotic effect on dentin, accelerating the degradation of hydrolytically unstable silane coupling silica [32]. Additionally, the degradation of the nanohybrid layer occurred, similar to previous SBU dentin bond durability studies [33]. The TEM morphological

images further supported this observation, revealing a loosened structure of the hybrid nanolayer at 6 months and the loss of integrity at the bottom of the hybrid layer at 1 year. Unlike previous research on SBU, the bond strength of ER-SUP did not show a significant decline with aging in the present study. SUP represents an improvement over SBU, with a new bottle having lower viscosity due to Bis-GMA free formulation and enhanced polymerization facilitated by the additional catalyst (data as detailed in the Material Safety Data Sheet provided by 3M ESPE). Therefore, the adhesive's lower viscosity and hydrophilic characteristics, combined with scrubbing activity during application, may enhance resin infiltration. Furthermore, the additional catalyst in the new bottle may improve the polymerization, collectively contributing to the integrity of the relatively thick hybrid layer. The TEM images illustrated a tight hybrid layer and banded collagen fibrils at 24 hours and 6 months, while the collagen fibrils were partially unraveled after 1 year. These findings correspond with a clinical trial study that displayed the durable bonding performance of SBU in ER mode [31]. However, a more extended investigation of SUP in ER mode is necessary.

In contrast, CPN(+) group exhibited a different outcome. No significant deterioration in bond strength was observed in either the MB2 or SUP group. Even though CPN was applied and then rinsed with distilled water before bonding application in SE mode, TEM

images still revealed platinum nanoparticles deposited along the exposed collagen fibrils of the hybrid layer. In this study, only the ER group was presented with the STEM/EDX mapping results, while the SE group was not included. This exclusion was due to the lower quantity of Pt nanoparticles in the SE group and the electron beam-induced damage, making it challenging to obtain accurate EDX mapping results. However, the platinum nanoparticles can still be observed in TEM morphological images in all SE groups. Previous studies suggested that CPN may play a critical role in promoting resin infiltration and increasing the conversion of the hybrid layer [21, 34]. It is noteworthy that the stability of Pt nanoparticles remained in the resin-dentin interface regardless of aging, appearing to preserve the integrity of hybrid layer. Furthermore, banded collagen fibrils attaching to platinum nanoparticles were observed in the aging group (Fig. 2e, f). Previous studies have demonstrated the inhibitory effect of platinum nanoparticles on matrix metalloprotease activity [35, 36]. Hence, the author speculated that CPN may play a role in preserving the integrity of collagen fibrils. However, the specific effect of CPN on the hybrid layer needs further study.

It has been reported that a concentration of 1 μg/ml platinum nanoparticles exhibits no cytotoxicity to fibroblast cells, and a concentration of 100 μg/mL platinum nanoparticles shows no cytotoxicity to normal cells [36]. Therefore, the CPN solution

used in the present study, with a platinum content of 0.02wt%, may demonstrate trustworthy biocompatibility. Future studies should explore various concentrations of platinum nanoparticles to better understand their impact on resin-dentin bonding durability and biosafety. Additionally, the average colloidal platinum particle size was around 2 to 3 nm (Fig. 5), which stabilizes with sodium citrate, enhancing surface reactivity due to the high surface area-to-volume ratio. Platinum nanoparticles remained on the dentin substrate even after rinsing. This phenomenon may be attributed to two factors. Firstly, colloidal-coated platinum nanoparticles may exhibit a hydrophilic tendency and high surface reactivity, similar to the hydrophilic nature of collagen fibrils. This similarity promotes the formation of attractive forces, enabling the nanoparticles to adhere to collagen fibrils. Secondly, platinum nanoparticles may interact with collagen fibrils through electrostatic attraction. Therefore, the findings of this study suggest that CPN application may contribute to enhancing the durability of resin-dentin bonding. However, further research is necessary to fully understand its specific effects and mechanisms.

5. Conclusion

This study revealed that the application of CPN significantly prevented degradation in the bond strength of MB2 and SE-SUP. However, no significant decrease was observed in

the bond strength of ER-SUP, either with aging or CPN application. The study also highlighted the potential inhibitory effect of CPN on the hydrolysis of collagen fibrils, as evidenced by TEM ultra-morphological images.

Overall, the findings suggest that CPN has the potential to enhance the durability of resin-dentin bonding, offering valuable insights for the development of adhesive systems in restorative dentistry. However, the specific function of CPN on the resin-dentin interface needs further investigation.

Acknowledgments

This study was supported by JST SPRING [grant number JPMJSP2119] and Grants-in-Aid for Scientific Research [project numbers. JP22H03271, JP21K19608] from the Japan Society for the Promotion of Science. The authors declared no potential conflicts of interest concerning the research, authorship, and/or publication of this article.

References

1. Nakabayashi N, Kojima K, Masuhara E. The promotion of adhesion by the infiltration of monomers into tooth substrates. J Biomed Mater Res 1982;16:265-73. https://doi.org/10.1002/jbm.820160307.
2. Koshiro K, Sidhu SK, Inoue S, Ikeda T, Sano H. New concept of resin-dentin interfacial adhesion: the nanointeraction zone. J Biomed Mater Res B Appl Biomater 2006;77:401-8. https://doi.org/10.1002/jbm.b.30450.
3. Van Meerbeek B, Yoshihara K, Van Landuyt K, Yoshida Y, Peumans M. From Buonocore's pioneering acid-etch technique to self-adhering restoratives. A status perspective of rapidly advancing dental adhesive technology. J Adhes Dent 2020;22:7-34. https://doi.org/10.3290/j.jad.a43994.
4. Mine A, De Munck J, Cardoso MV, Van Landuyt KL, Poitevin A, Kuboki T, et al. Bonding effectiveness of two contemporary self-etch adhesives to enamel and dentin. J Dent 2009;37:872-83. https://doi.org/10.1016/j.jdent.2009.06.020.

5. Van Meerbeek B, Yoshihara K, Yoshida Y, Mine AJ, De Munck J, Van Landuyt KL. State of the art of self-etch adhesives. Dent mater 2011;27:17-28. https://doi.org/10.1016/j.dental.2010.10.023.
6. Da Rosa WL, Piva E, da Silva AF. Bond strength of universal adhesives: a systematic review and meta-analysis. J Dent 2015;43:765-76. https://doi.org/10.1016/j.jdent.2015.04.003.
7. Breschi L, Mazzoni A, Ruggeri A, Cadenaro M, Di Lenarda R, Dorigo ED. Dental adhesion review: aging and stability of the bonded interface. Dent mater 2008;24:90-101. https://doi.org/10.1016/j.dental.2007.02.009.
8. Tjäderhane, L. Dentin bonding: can we make it last?. Oper Dent 2015;40:4-18. https://doi.org/10.2341/14-095-BL.
9. Rao CN, Cheetham AK. Science and technology of nanomaterials: current status and future prospects. J Mater Chem 2001;11:2887-94. https://doi.org/10.1039/B105058N.
10. AlKahtani RN. The implications and applications of nanotechnology in dentistry: a review. The Saudi Dent J 2018;30:107-16. https://doi.org/10.1016/j.sdentj.2018.01.002.

11. Jandt KD, Watts DC. Nanotechnology in dentistry: present and future perspectives on dental nanomaterials. Dent Mater 2020;36:1365-78. https://doi.org/10.1016/j.dental.2020.08.006.

12. Carrouel F, Viennot S, Ottolenghi L, Gaillard C, Bourgeois D. Nanoparticles as anti-microbial, anti-inflammatory, and remineralizing agents in oral care cosmetics: a review of the current situation. Nanomaterials (Basel) 2020;10:140. https://doi.org/10.3390/nano10010140.

13. Lin CS, Khan MR, Lin SD. The preparation of Pt nanoparticles by methanol and citrate. J Colloid Interface Sci 2006;299:678-85. https://doi.org/10.1016/j.jcis.2006.03.003.

14. Kajita M, Hikosaka K, Iitsuka M, Kanayama A, Toshima N, Miyamoto Y. Platinum nanoparticle is a useful scavenger of superoxide anion and hydrogen peroxide. Free Radic Res 2007;41:615-26. https://doi.org/10.1080/10715760601169679.

15. Watanabe A, Kajita M, Kim J, Kanayama A, Takahashi K, Mashino T, et al. In vitro free radical scavenging activity of platinum nanoparticles. Nanotechnology 2009;20:455105. https://doi.org/10.1088/0957-4484/20/45/455105.

16. Onizawa S, Aoshiba K, Kajita M, Miyamoto Y, Nagai A. Platinum nanoparticle antioxidants inhibit pulmonary inflammation in mice exposed to cigarette smoke. Pulm Pharmacol Ther 2009;22:340-9. https://doi.org/10.1016/j.pupt.2008.12.015.

17. Bendale Y, Bendale V, Paul S. Evaluation of cytotoxic activity of platinum nanoparticles against normal and cancer cells and its anticancer potential through induction of apoptosis. Integr Med Res 2017;6:141-8. https://doi.org/10.1016/j.imr.2017.01.006.

18. Hashimoto M, Kawai K, Kawakami H, Imazato S. Matrix metalloproteases inhibition and biocompatibility of gold and platinum nanoparticles. J Biomed Mater Res A 2016;104:209-17. https://doi.org/10.1002/jbm.a.35557.

19. Pedone D, Moglianetti M, De Luca E, Bardi G, Pompa PP. Platinum nanoparticles in nanobiomedicine. Chem Soc Rev 2017;46:4951-75. https://doi.org/10.1039/C7CS00152E.

20. Zhang H, Hasebe A, Alam A, Liu Y, Hoshika S, Yamauti M, Sano H. Antibacterial potential of colloidal platinum nanoparticles against *Streptococcus mutans*. Dent Mater J 2022;41:368-75. https://doi.org/10.4012/dmj.2021-203.

21. Hashimoto M, Yanagiuchi H, Kitagawa H, Honda Y. Inhibitory effect of platinum nanoparticles on biofilm formation of oral bacteria. Nano Biomed 2017;9:77-82. https://doi.org/10.11344/nano.9.77.

22. Hoshika S, Nagano F, Tanaka T, Wada T, Asakura K, Koshiro K, et al. Expansion of nanotechnology for dentistry: effect of colloidal platinum nanoparticles on dentin adhesion mediated by 4-META/MMA-TBB. J Adhes Dent 2011;13:411-6. https://doi.org/10.3290/j.jad.a19818.

23. Armstrong S, Breschi L, Özcan M, Pfefferkorn F, Ferrari M, Van Meerbeek B. Academy of Dental Materials guidance on in vitro testing of dental composite bonding effectiveness to dentin/enamel using micro-tensile bond strength (μTBS) approach. Dent Mater 2017;33:133-143. https://doi.org/10.1016/j.dental.2016.11.015

24. Sano H, Chowdhury AFMA, Saikaew P, Matsumoto M, Hoshika S, Yamauti M. The microtensile bond strength test: Its historical background and application to bond testing. Jap Dent Sci Rev 2020;56:24-31. https://doi.org/10.1016/j.jdsr.2019.10.001

25. Yoshihara K, Yoshida Y, Nagaoka N, Hayakawa S, Okihara T, De Munck J, et al. Adhesive interfacial interaction affected by different carbon-chain monomers. Dent Mater 2013;29:888-97. https://doi.org/10.1016/j.dental.2013.05.006.

26. Yoshida Y, Yoshihara K, Nagaoka N, Hayakawa S, Torii Y, Ogawa T, et al. Self-assembled nano-layering at the adhesive interface. J Dent Res 2012;91:376-81. https://doi.org/10.1177/0022034512437375.

27. Yoshihara K, Nagaoka N, Okihara T, Kuroboshi M, Hayakawa S, Maruo Y, et al. Functional monomer impurity affects adhesive performance. Dent Mater 2015;31:1493-501. https://doi.org/10.1016/j.dental.2015.09.019.

28. Zhou J, Tan J, Chen L, Li D, Tan Y. The incorporation of chlorhexidine in a two-step self-etching adhesive preserves dentin bond in vitro. J Dent 2009;37:807-12. https://doi.org/10.1016/j.jdent.2009.06.011.

29. Takamizawa T, Hirokane E, Sai K, Ishii R, Aoki R, Barkmeier WW, et al. Bond durability of a two-step adhesive with a universal-adhesive-derived primer in different etching modes under different degradation conditions. Dent Mater J 2023;42:121-32. https://doi.org/10.4012/dmj.2022-130.

30. Wagner A, Wendler M, Petschelt A, Belli R, Lohbauer U. Bonding performance of universal adhesives in different etching modes. J Dent 2014;42:800-7. https://doi.org/10.1016/j.jdent.2014.04.012.

31. Lawson NC, Robles A, Fu CC, Lin CP, Sawlani K, Burgess JO. Two-year clinical trial of a universal adhesive in total-etch and self-etch mode in non-carious cervical lesions. J Dent 2015;43:1229-34. https://doi.org/10.1016/j.jdent.2015.07.009.

32. Kawazu M, Takamizawa T, Hirokane E, Tsujimoto A, Tamura T, Barkmeier WW, et al. Comparison of dentin bond durability of a universal adhesive and two etch-and-rinse adhesive systems. Clin Oral Investig 2020;24:2889-97. https://doi.org/10.1007/s00784-019-03153-y.

33. de Paris Matos T, Perdigao J, De Paula E, Coppla F, Hass V, Scheffer RF, et al. Five-year clinical evaluation of a universal adhesive: a randomized double-blind trial. Dent Mater 2020;36:1474-85. https://doi.org/10.1016/j.dental.2020.08.007.

34. Matinlinna JP, Lung CY, Tsoi JK. Silane adhesion mechanism in dental applications and surface treatments: a review. Dent Mater 2018;34:13-28. https://doi.org/10.1016/j.dental.2017.09.002.

35. Zhang ZY, Tian FC, Niu LN, Ochala K, Chen C, Fu BP, et al. Defying ageing: an expectation for dentine bonding with universal adhesives?. J Dent 2016;45:43-52. https://doi.org/10.1016/j.jdent.2015.11.008.

36. Katsumata A, Katsumata T, Hoshika S, Hoshika T, Nishitani T, Yajima T, et al. Dentin bond strength of the universal adhesives using the colloidal platinum nanoparticles. J Oral Tissue Engin 2017;15:11-7. https://doi.org/10.11223/jarde.15.11.

37. Hashimoto M, Yamaguchi S, Sasaki JI, Kawai K, Kawakami H, Iwasaki Y, et al. Inhibition of matrix metalloproteinases and toxicity of gold and platinum nanoparticles in L929 fibroblast cells. Eur J Oral Sci 2016;124:68-74. https://doi.org/10.1111/eos.12235.

38. Hashimoto M, Kawai K, Kawakami H, Imazato S. Matrix metalloproteases inhibition and biocompatibility of gold and platinum nanoparticles. J Bio Mater Res A 2016;104(1):209-17. https://doi.org/10.1002/jbm.a.35557.